

1 'Revised article – clean copy'

2 **The impact of combinatorial stress on the growth dynamics and metabolome of *Burkholderia***
3 ***mesoacidophila* demonstrates the complexity of tolerance mechanisms**

4 **Suzy Clare Moody^{1,2}, James C. Bull¹, Ed Dudley³ and E. Joel Loveridge¹**

5 **1.** College of Science, Swansea University, Swansea, UK, SA2 8PP.


6 **2.** School of Sport, Health and Social Science, Solent University, Southampton, UK, SO14 0YN.

7 **3.** College of Medicine, Swansea University, Swansea, UK, SA2 8PP.

8 **Running title: Growth dynamics *B. mesoacidophila***

9 Corresponding authors:

10 Suzy Clare Moody, suzy.moody@solent.ac.uk. School of Sport, Health and Social Science, Solent

11 University, Southampton, UK, SO14 0YN. Tel: 

12 E. Joel Loveridge, e.j.loveridge@swansea.ac.uk. College of Science, Swansea University, Swansea,

13 UK, SA2 8PP. Tel: 

14

15 **Abstract**

16 Aims: The recently sequenced *Burkholderia mesoacidophila* (previously *Pseudomonas*
17 *mesoacidophila*) is a soil organism and as such will be exposed to multiple concurrent stresses in the
18 natural environment. The combinatorial stress potentially experienced by microbes in soil has not
19 been investigated in detail.

20 Methods and Results: The impact of combinatorial stress on growth was investigated using tripartite
21 variables – temperature, nutritional environment and either osmotic or oxidative stress. In
22 nutritionally stringent conditions, increasing diamide concentration had no effect on growth while
23 increasing H₂O₂ concentration reduced both growth rate and maximum density. Metabolomic
24 studies with oxidative stress revealed specific (unidentified) metabolites associated with diamide
25 tolerance, and an overwhelming dominance of sugars and sugar alcohols in nutritionally stringent
26 conditions with and without the additional stressor.

27 Conclusions: Combinatorial stress tolerance is complex. Temperature had the greatest independent
28 impact on growth, while the impact of the nutritional environment played a key role in oxidative
29 stress tolerance. In nutritionally stringent conditions, the metabolome suggested different tolerance
30 mechanisms for different types of oxidative stress.

31 Significance and Impact of Study: This work demonstrates the specificity of the stress response, and
32 the need to consider multiple environmental factors to meaningfully investigate tolerance. Both
33 environmental and clinical settings subject bacteria to combinatorial stress and this should be
34 considered in the design of further studies.

35 Keywords: stress tolerance; *Burkholderia*; growth dynamics; metabolome; diamide; oxidative stress

36 **Introduction**

37 *Burkholderia mesoacidophila* (the proposed new name for the species previously called
38 *Pseudomonas mesoacidophila*) is a soil organism which belongs to the *Burkholderia cepacia* complex
39 (Bcc; Loveridge *et al.*, 2017) and is therefore of both environmental and potentially clinical interest.
40 Organisms in all ecological niches experience stressful conditions sometimes. Bacteria, as single
41 celled organisms, are both uniquely vulnerable to environmental change and exquisitely well-
42 adapted to rapid metabolic adaptation to enable survival. *B. mesoacidophila* was originally identified
43 from soil samples (Imada *et al.*, 1981), and yet there is a paucity of further information about its
44 ecology and growth dynamics. Its genome has recently been sequenced, and shows considerable
45 potential for specialised metabolite production (Loveridge *et al.*, 2017). Specialised metabolites are
46 often associated with growth in stressful conditions, but little is currently known about the stress
47 tolerances of this under-studied species and it has not yet been characterised in terms of metabolic
48 potential. As these specialised metabolites may be utilised in industrial or therapeutic settings, the
49 effect of stress on *B. mesoacidophila* is of general interest.

50 Osmotic stress and oxidative stress are experienced by bacteria in both the clinical and
51 environmental setting and must be tolerated or ameliorated. Some studies of a variety of stress
52 responses in the Burkholderiaceae have been conducted. In an elegant study of osmotic stress,
53 Behrends *et al.* (2011) showed a decrease in culture optical density and an increase of glycine-
54 betaine and/ or trehalose concentration in response to 0.5 mol l⁻¹ NaCl in a range of strains of
55 *Burkholderia cenocepacia*. The study highlighted that assumptions of parity across the genus are
56 unwise as they also demonstrated a wide range of inter-strain variability. Pumirat *et al.* (2009) also
57 used a salt stress (of 150 mmol l⁻¹ NaCl) to study the impact on the secretome of *Burkholderia*
58 *pseudomallei*, showing changes in proteins associated with metabolic pathways, solute transport
59 and drug resistance amongst others. The impact on growth was not reported. A comprehensive
60 study into the effects of several different stressors on survival and growth of *B. pseudomallei*
61 demonstrated how robust some members of this genus can be (Robertson *et al.*, 2010), but did not
62 combine stresses or investigate the mechanisms of survival. Pumirat *et al.* (2017) used exposure to a

63 range of salt concentrations to prime *B. pseudomallei* cultures before challenge with either high
64 temperature or oxidative stress (mediated by H₂O₂), and an increase in thermo- and oxidative stress
65 tolerance was seen. Further studies have highlighted susceptibility to oxidative stress as being a
66 function of growth temperature (Paksanont *et al.*, 2018). These last two studies highlight the
67 potential for co-ordination of stress tolerance mechanisms across different specific stress-inducing
68 conditions, and the inter-dependence of stress responses in enabling growth in challenging
69 conditions. This reinforces the need for studies utilising multiple concurrent stressors to gain a true
70 understanding of the survival ability of this hardy genus.

71 This study therefore aims to further this field by considering the impact of exposure to simultaneous,
72 multiple stressors, which is more likely to be how stress is experienced in the soil environment. The
73 stresses chosen are known in other species to exhibit some features of co-regulation (e.g. ScbR2 in
74 *Streptomyces coelicolor*, Li *et al.*, 2015; σ^B in *Listeria monocytogenes*, Liu *et al.*, 2017) and are known
75 to interact and act on some of the same pathways or processes in the cell. General oxidative stress
76 was simulated here with the addition of an increasing concentration of H₂O₂ to the media. This
77 exposes cells to free radicals and reactive oxygen species (ROS) which damage proteins, DNA and
78 lipids. A particular example of oxidative stress is a disulphide stress, caused by the addition of
79 diamide to the media. Diamide is a membrane-permeable oxidizer which targets protein cysteine
80 thiol groups, causing disulphide bridges to form, ultimately leading to both a redox imbalance and
81 potential protein misfolding (Kallifidas *et al.*, 2010). Osmotic stress is simulated by the addition of
82 KCl to the media, and the impact that has on water availability within the cell.

83 These three stresses were applied individually at a range of concentrations. Each stress condition
84 was tested in two different media conditions, one a nutrient rich environment (Luria Bertani, LB) and
85 the other a more limited nutrient broth (Czapek-Dox, CD). CD broth is a sucrose-based medium
86 containing 35 mmol l⁻¹ sodium nitrate. The recently sequenced genome suggests *B. mesoacidophila*
87 has genetic capacity to assimilate and metabolise both sucrose and nitrate/nitrite, and previous

88 work has demonstrated both reduction of nitrates and utilisation of inorganic nitrogen sources
89 (Kintaka *et al.*, 1981). Further work on related species suggests nitrate is a preferred nitrogen source
90 at a concentration of at least 10 mmol l⁻¹ and therefore nitrogen availability is unlikely to be limiting
91 to growth (Lardi *et al.*, 2015; Mangalea *et al.*, 2017). It was anticipated therefore that this medium
92 would present a more stringent nutritional environment while providing both carbon and nitrogen in
93 a usable form. The experimental work was then conducted at four different temperatures ranging
94 from a warm environmental temperature (25 °C) to that associated with pathogenicity in humans
95 (40 °C). Thus the tripartite combination of nutritional availability, temperature challenge and added
96 stressor was investigated. Although liquid culture does not necessarily inform on behaviour in soil or
97 the clinic, it was used here as larger scale production and metabolite extraction would be more
98 feasible if interesting specialised metabolites were detected (although that is beyond to scope of the
99 current work). The results show that *B. mesoacidophila* can tolerate a wide range of growth
100 conditions, and that nutritional availability has a differential impact on stress tolerance.

101 **Materials and Methods**

102 **Microbial culture and plate reader set-up**

103 *B. mesoacidophila* (ATCC 31433) overnight cultures were grown in 5 ml LB low salt broth, incubated
104 at 30 °C and 150 rpm, to an optical density of 0.2 at 550 nm. 20 µl of overnight culture was added to
105 each well, with 180 µl of the appropriate test media. All plates were run for 24 hours in a
106 ThermoScientific Multiskan FC, shaken for 10 seconds prior to a reading at 550 nm every hour. Two
107 media with different nutritional content were used – low salt LB broth and CD broth (Sigma)
108 amended with KCl (Fisher) with give a total molarity of 85.5 mmol l⁻¹ salt, which is equivalent to the
109 LB. Osmotic stress was induced using the addition of KCl to these baseline media to give a range of
110 total salt molarities from 85.5 mmol l⁻¹ to 375 mmol l⁻¹. (Unamended CD was also used in the
111 osmotic stress experiment, which has 6.7 mmol l⁻¹ KCl.) Oxidative stress was induced by the addition
112 of H₂O₂ (Fisher) at concentrations ranging from 88 µmol l⁻¹ to 880 µmol l⁻¹. Disulphide stress was

113 induced using a range of diamide (Fisher) concentrations from 1 mmol l⁻¹ to 0.125 mmol l⁻¹. Each
114 experiment was conducted at four temperatures: 25, 30, 37 and 40 °C. All experiments were
115 conducted in triplicate, with blank media controls also in triplicate for all conditions.

116 **Statistical analysis of growth dynamics**

117 Growth curves were initially visualised using Generalised Additive Mixed Models (GAMMs) with
118 cubic spline smoothing functions. Changes in optical density (the response variable) were modelled
119 over time, due to variation in both temperature stress and chemical stressor concentration (i.e.,
120 time x temperature + time x concentration). Since each of the three types of chemical stressor was
121 applied over differing ranges of concentrations, this was done separately for each stressor. This
122 analysis was performed for each growth medium (LB and CD). Replicates grouped by experimental
123 plates were modelled as random intercepts, temporal autocorrelation was modelled as a first-order
124 autoregressive process (AR1), and Gaussian residual errors were assumed (and verified by visual
125 inspection). Results were visualised graphically for each stressor (temperature and chemical
126 concentration) while averaging across the effects of the third stressor.

127 Having identified the underlying functional form of the dynamics using smoothing splines, logistic
128 growth curves were subsequently fitted to individual combinations of temperature stress and
129 chemical stressor concentration using Nonlinear Mixed-Effects Models (NLMEs) with the same
130 random effects and variance-covariance structure as described above for GAMMs. This allowed
131 estimation of averages and 95 % confidence intervals for the asymptote (growth curve plateau),
132 midpoint (time at which optical density reaches 50 % of the maximum), and scale parameter
133 (relating to the slope of the logistic curve at the midpoint, so maximum growth rate) for each
134 treatment combination. This approach permitted statistical comparison of growth dynamics
135 between treatments.

136 **Culture for metabolite extractions**

137 For metabolite extractions, cultures were inoculated with 100 μ l of fresh overnight culture (as
138 described in the section above) into 5 ml CD85, CD85 with 220 μ mol l⁻¹ H₂O₂ or CD85 with 1 mmol l⁻¹
139 diamide. The cultures were incubated at 30 °C, 200 rpm for 20 hours. All conditions were conducted
140 in triplicate.

141 **Metabolite quenching and extraction**

142 The cultures were harvested by centrifugation at 4500 x *g* for 10 minutes at room temperature. The
143 supernatant was decanted, and the remaining cell pellet was flash frozen under liquid N₂. 1 ml
144 methanol (Fisher) was added and the samples were then sonicated in a cool water bath for 1 hour
145 with vortexing part way through to ensure good cell breakage. All samples were centrifuged at 4500
146 x *g* for 5 minutes at room temperature. The solvent layer was removed into separate tubes and
147 dried *in vacuo*.

148 **GC-MS analysis**

149 The dried samples were derivatized to increase volatility, according to the following methodology:
150 the dried samples were dissolved in 30 μ l of 15 mg/ml methoxyamine in pyridine and baked for 60
151 minutes at 70 °C. 50 μ l of MSTFA (N-Methyl-N-(trimethylsilyl) trifluoroacetamide) was added, and
152 the samples were incubated at 40 °C for 90 minutes. The samples were run on an Agilent HP5975C
153 GC-MS, using a 1 μ l injection volume and a Durabond DB-5 column (length 30 m, diameter 0.25 mm
154 with a 0.25 μ m film) with helium as the carrier gas. The column temperature was held at 50 °C for 2
155 minutes, increased to 300 °C at 10 °C /min, then held for a further 15 minutes at 300 °C . Mass
156 spectra were acquired using an electron impact ion source with an emission voltage of 70 eV, single
157 quadrupole ion separation and detection between 50 and 600 amu. Results were analysed using
158 OpenChrom and the NIST database.

159 **Results**

160 **Growth dynamics during combinatorial stress**

161 To investigate the impact of multiple concurrent stressors on growth rate and maximum cell density,
162 growth curves were set up using LB and CD85 broth. Both media have a pH of approximately 7, so
163 acidity/alkalinity was not considered as an added variable. The 24 hour incubation time enabled
164 logarithmic growth and entry into stationary phase when the bacteria were in control conditions in
165 both media. As anticipated, LB consistently represented a nutritionally replete environment and as
166 such, supported a higher maximum cell density than CD85. This simpler medium provided a more
167 nutritionally stringent environment, appearing to provide sufficient usable carbon and nitrogen to
168 support growth but with a reduced end-point density, suggesting some growth limitation. The
169 additional stressors tested in conjunction with nutritional availability were temperature (range 25-40
170 °C), salt concentration (85.5 mmol l⁻¹ to 375 mmol l⁻¹) and oxidative stress (0.125 mmol l⁻¹ to 1 mmol
171 l⁻¹ diamide or 88 μmol l⁻¹ to 880 μmol l⁻¹ H₂O₂). *B. mesoacidophila* showed optimal growth at 30 °C in
172 both nutritional conditions, and barely grew at higher temperatures. Thermotolerance was such a
173 strong factor that when temperature was high, neither of the other two stressors (nutrient
174 availability or chemical stressor) had an additional effect (R side panel of both Figures 1 and 2). In
175 contrast, nutrient availability was a strong predictor for maximum optical density reached at 25 °C
176 and 30 °C, with the limited nutritional environment limiting cell density. (At 37 °C and 40 °C the
177 additional nutrient availability did not overcome the effect of temperature and cultures grew equally
178 poorly.)

179 **Stress tolerance in nutritionally replete conditions**

180 In nutritionally replete conditions, while *B. mesoacidophila* was able to grow well at 25 °C, 30 °C
181 remained the overall optimal temperature for both growth rate and final optical density for all three
182 additional stressors (Figure 1, R panel). The salt tolerance experiments (Figure 1, top row) revealed
183 optimal growth occurred at 125 mmol l⁻¹ total salt concentration. Unamended LB media contained
184 sufficient salt (85.5 mmol l⁻¹) for this never to be a limiting factor at low concentration, and salt
185 tolerance with minimal impact on growth was observed at 250 mmol l⁻¹. At 375 mmol l⁻¹ a

186 substantial drop in final cell density was noted, at both 25 °C and 30 °C. Using an oxidative stress
187 induced by either H₂O₂ or diamide failed to impact on the growth rate or final optical density of *B.*
188 *mesoacidophila*, even at the highest concentration (880 μmol l⁻¹ or 1 mmol l⁻¹ respectively, Figure 1,
189 middle and bottom rows).

190 **Stress tolerance in nutritionally stringent conditions**

191 In nutritionally stringent conditions, growth was consistently best at 30 °C across all stress conditions
192 but response to temperature as one of multiple stresses was neither consistent nor predictable
193 (Figure 2, R panel). It was noted that during combined nutritional and oxidative stress (induced by
194 either H₂O₂ or diamide) that temperature tolerance had a narrow range, with poor growth at 25 °C,
195 37 °C and 40 °C (Figure 2, R panel, top and bottom rows). This was in contrast to the data obtained
196 using nutritional and osmotic stress, which suggested low level salt supplementation (85.5 mmol l⁻¹
197 and 175 mmol l⁻¹) enabled comparable growth and cell densities at 25 °C and 30 °C (Figure 2, R
198 panel, middle row). Growth was still poor at 37 °C and 40 °C, regardless of salt concentration.

199 At the optimal temperature of 30 °C, there were differences noted in combined stress tolerance
200 based on the concentration of the chemical stressor. In osmotically challenging conditions, a great
201 deal of variation was seen, with both salt stringency and salt overload suggested in the data. At low
202 salt concentration (unamended CD has a salt concentration of 6.7 mmol l⁻¹), growth was as limited as
203 it was at high salt concentration (Figure 2, L panel, middle row). No impact on growth rate or final
204 optical density was seen with diamide supplementation (Figure 2, L panel, top row). This was in
205 contrast to the other source of oxidative stress used, H₂O₂, which showed a decrease in maximum
206 optical density with increasing concentration at 30 °C (Figure 3).

207 **Statistical comparison of stress tolerance in the two nutritional conditions**

208 Statistical analysis of these results using the logistic growth model showed that the asymptote for
209 both media was highest at intermediate salt concentrations, confirming that the selection of
210 concentrations spanned the tolerance range for *B. mesoacidophila*.

211 When subjected to increasing diamide stress, the impact on growth rate (measured as the midpoint
212 of the curve) was small but negative, more so in the richer medium. The maximum optical density
213 achieved was consistently higher in LB. More of a surprise was the finding that in LB maximum
214 growth decreases with increasing diamide concentration, whereas this is not seen when grown in
215 CD85. Broadly speaking, diamide stress did not have a big effect on growth as part of the
216 combinatorial stress set-up, and nutritional availability had far more impact and was more limiting
217 than diamide.

218 When exposed to H₂O₂, as in the diamide treatment, the asymptote was higher in LB than CD85. In
219 contrast to the diamide data, maximum growth in H₂O₂ treated cells decreased with increasing H₂O₂
220 in CD85 but not in LB, indicating a potential reduction in H₂O₂ stress tolerance during nutritionally
221 stringent conditions. The midpoint of growth (indicative of growth rate) was similar in both media
222 and decreased with increasing H₂O₂ concentration.

223 In summary, *B. mesoacidophila* growth is reduced in CD85 compared to LB but the response to
224 oxidative stress in CD85 varies with which stressor is used, suggesting different pathways to
225 tolerance.

226 **Metabolomics of combinatorial stress**

227 The growth dynamics data were used to identify conditions in which *B. mesoacidophila* could grow
228 exponentially and enter stationary phase within a 20 hour time frame. Growth was inhibited in CD85
229 compared to LB, suggestive of a degree of nutritional stress. A total salt concentration of 85 mmol l⁻¹
230 in CD media was permissive for our growth requirements, while being sub-optimal for growth (as
231 shown in the growth dynamics experiments). The CD media amended to 85 mmol l⁻¹ total salt (CD85)

232 was chosen as a baseline media, for enabling sufficient growth to sample without being optimal in
233 terms of nutritional content or salt concentration. The impact of diamide on growth in CD85 at 30 °C
234 was shown above to be negligible, while the impact of H₂O₂ was considerable. These were therefore
235 followed up at concentrations which had an impact on cell density but still allowed log growth and
236 entry into stationary phase within 20 hours. Intracellular metabolites were extracted from cells
237 grown in CD85, CD85 with 1 mmol l⁻¹ diamide and CD85 with 220 µmol l⁻¹ H₂O₂, and derivatised with
238 MSTFA to increase the volatility of molecules such as alcohols (including simple sugars) and
239 carboxylic acids. Derivatised samples were analysed by GC-MS to identify any differences that may
240 be associated with the tolerance of diamide and the stress induced by H₂O₂.

241

242 The majority of GC-MS peaks putatively identifiable with a NIST score of 80 or higher were sugars
243 (Figure 4 and Supplementary Information Table S1), and the remainder were sugar alcohols (glycerol
244 and xylitol) and a carboxylic acid (gluconic acid). Glycerol and glucose were detected in all samples,
245 mannose in all but one CD85 with H₂O₂ sample (Figure 5 and Supplementary information Table S2).
246 Analysis of the relative abundance of the sugars and related alcohols was performed, based on the
247 raw peak areas in the total ion current chromatogram. In all samples, simple sugars (glucose and
248 mannose) were the dominant metabolites detected, by three or four orders of magnitude. Gluconic
249 acid was detected in greater abundance than glycerol only in the CD85 samples. Diamide treatment
250 did not lead to significant changes in the concentrations of any metabolite identified, although the
251 relative proportion of xylitol to glycerol increased significantly, whereas H₂O₂ treatment led to a
252 10±2-fold increase in the amount of glycerol. The samples contained between 10 and 15 unique
253 compound peaks (excluding peaks for different derivatives of the same parent compound and
254 multiple peaks identifying the same compound, within the constraints of robust NIST identification).
255 Diamide treated samples uniquely and reproducibly contained two small peaks – one at 7.142

256 minutes, and one at approximately 53 minutes (Figure 6), neither of which was identifiable using the
257 NIST database.

258 The H₂O₂ treated samples were less consistent, perhaps suggestive of a more disordered metabolic
259 response to stress. In one sample (#2) 2 keto-l-gluconic acid was putatively identified with a NIST
260 score of 64, but not seen in either of the other replicates. The same #2 sample also putatively
261 contained butanal (NIST score 80), which was not seen in any other samples. Sample #3 uniquely
262 contained a tentatively identified 3-O-β-d-mannopyranosyl-d-glucitol (NIST score 64). None of these
263 compounds were identified in the CD85 samples or diamide samples.

264 **Discussion**

265 This work is one of few to examine the role of combinatorial stress on growth dynamics and the
266 metabolome in *Burkholderia*. Uniquely the impact of a range of each factor has been studied,
267 enabling a more global view of the impact of stress on growth. Thermo-tolerance has been shown to
268 be the strongest determinant of *B. mesoacidophila* growth, with a strong preference for 25-30 °C
269 temperature range, and extremely inhibited growth above that. This suggests this species has
270 limited human pathogenic potential due to temperature tolerance, despite being part of the Bcc. In
271 contrast to *B. pseudomallei* (Pumirat *et al.*, 2017) the presence of salt in the medium did not impact
272 on thermo-tolerance, and nor did nutritional stress. While the asymptote was lower in nutritionally
273 stringent conditions in all experiments, the salt tolerance range was comparable to that in rich
274 media and no major differences in thermo-tolerance were observed. This may be due to the stresses
275 being experienced combinatorially in this work but sequentially in the aforementioned study.

276 Tolerance of oxidative stress was variable depending on both the type of oxidative stress used and
277 the nutritional conditions. While the range of diamide concentrations used here did not show an
278 impact on *B. mesoacidophila* growth dynamics in either of the nutritional conditions or in terms of
279 an additive effect on temperature tolerance, differences were seen in the metabolome profile. Two

280 unique peaks were identified in the diamide spiked cultures which were absent in all other samples.
281 Although they remain unidentified, their presence suggests induction of tolerance pathways
282 enabling normal growth to continue. Tolerance to diamide is typically mediated by NADPH-
283 dependent thioredoxins reducing damaged disulphides (Chavarria *et al.*, 2012), but this work may
284 also indicate production of new, protective metabolites. Additionally, the relative abundance of
285 xylitol in the diamide treated cells is interesting as xylose metabolism has been shown to be
286 impacted by the presence of diamide in yeast. Hector *et al.* (2011) found that at concentrations
287 which did not impact negatively on growth, diamide treatment up-regulated genes involved in xylose
288 metabolism. This would be an interesting avenue for future work.

289 In contrast, using an oxidative stress induced by the presence of H₂O₂ did show an impact on growth
290 when under nutritionally stringent conditions. Previous work on this strain (originally identified as
291 *Pseudomonas mesoacidophila* strain SB-72310) characterised its ability to produce catalase in
292 response to H₂O₂ challenge (Kintaka *et al.*, 1981) but did not report the effect on growth. In this
293 work, when nutritionally replete the wide range of H₂O₂ concentrations used did not have an impact
294 on asymptote, although it did reduce the midpoint – indicative of a decrease in growth rate, even if
295 the same final cell density was still achieved. When grown in nutritionally stringent conditions, the
296 same effect was seen with a gradual reduction in the midpoint with increasing H₂O₂ concentration,
297 but there was also a significant decline in asymptote at the higher concentrations of H₂O₂ suggesting
298 a failure of tolerance mechanisms to mitigate against generalised oxidative damage. This, combined
299 with the metabolomics, suggests that the pathways induced to tolerate oxidative stress may be
300 different depending on the type of oxidative damage the cell experiences.

301 The mechanisms of oxidative stress tolerance pathway induction are complex with multiple
302 transcription factors identified as important (e.g. σ E, Jitprasutwit *et al.*, 2014; OxyR, Si *et al.*, 2017)
303 and functional redundancy built in to the proteome (e.g. Reott *et al.*, 2009). The genome of *B.*
304 *mesoacidophila* encodes a range of predicted proteins with known roles in protection such as

305 superoxide dismutase, catalases, peroxidases and thiol peroxidases (Loveridge *et al.*, 2017). The
306 roles of glutathione and thioredoxin in protection against oxidative stress are well established
307 (Carmel-Harel and Storz, 2000) as both systems contribute to the continuance of a reduced
308 intracellular environment. Evidence suggests that within this group of protective proteins,
309 differential induction and expression can be seen on exposure to either diamide or H₂O₂ as a source
310 of stress (Somprasong *et al.*, 2012). Viewing the results presented here through the lens of this prior
311 knowledge suggests that combinatorial stress including nutritional stringency may have a disruptive
312 effect on these processes, with greater impact seen in a generalised stress response. While the cell
313 induced production of novel, possibly protective metabolites in response to diamide, the same co-
314 ordination of an effective stress response was not seen in the H₂O₂ metabolomics.

315 The metabolomic studies were conducted in a nutritionally stringent environment, with sub-optimal
316 salt concentration (85 mmol l⁻¹) and either 1 mmol l⁻¹ diamide or 220 µmol l⁻¹ H₂O₂, thereby
317 subjecting the cells to a tripartite combinatorial stress. The metabolites detected at the highest
318 concentration and in all samples were glycerol and glucose, with mannose detected in all but one
319 sample (CD85 with H₂O₂). Previous work has shown *B. mesoacidophila* (identified as strain SB-72310)
320 to assimilate and grow on all three of these compounds as the sole carbon source (Kintaka *et al.*,
321 1981). Glucose is the most abundant monosaccharide in biological systems, so its presence in
322 relatively high abundance is to be expected. The sugar alcohol glycerol (synonym glycerin) is an
323 intermediate in carbohydrate and lipid metabolism. It has also been identified as part of the
324 endogenous stress response in bacteria (Chen *et al.*, 2017), and conducive to thermotolerance of
325 *Pseudomonas* when applied exogenously (Srivastava *et al.*, 2008). Previous evidence also suggests
326 both glycerol and glucose may be accumulated by *Pseudomonas putida* and *Pseudomonas*
327 *fluorescens* during salt stress (Sévin *et al.*, 2015). The ubiquitous presence of glycerol in the
328 metabolome of *B. mesoacidophila* growing under tripartite stress is therefore unsurprising.
329 Mannose and mannose-derived compounds have been shown to be important in production of

330 protective exopolysaccharides and to confer tolerance to ROS (Ge *et al.*, 2013; Cuzzi *et al.*, 2014) and
331 contribute to osmoregulation (Smith *et al.*, 1990).

332 In summary, while models of genomic similarity may cluster species together in the Bcc, this hides a
333 wealth of diversity in terms of tolerance and ability to survive adverse conditions. Individual species
334 are worthy of investigation to understand growth dynamics and no assumptions can be made about
335 common stress tolerance pathways and processes. Combinatorial stress is likely to be encountered
336 in the natural environment, either in a human host or in soil, and studies must therefore consider
337 the impact of multiple stresses on the growth and survival of *Burkholderia* species.

338 Acknowledgements: We thank the Life Sciences Research Network Wales for funding this work
339 through grant NRNRG4Mar039. We thank the reviewers and editorial team for their constructive
340 comments and suggested improvements to the manuscript.

341 Conflict of Interest: The authors declare no conflict of interest.

342 **References**

343 Behrends V, Bundy JG, Williams HD. Differences in strategies to combat osmotic stress in
344 *Burkholderia cenocepacia* elucidated by NMR-based metabolic profiling. Lett Appl Microbiol. 2011
345 Jun;52(6):619-25. doi: 10.1111/j.1472-765X.2011.03050.x. Carmel-Harel O, Storz G. Roles of the
346 glutathione- and thioredoxin-dependent reduction systems in the *Escherichia coli* and
347 *Saccharomyces cerevisiae* responses to oxidative stress. Annu Rev Microbiol. 2000;54:439-61.
348 Chavarría M, Nikel PI, Pérez-Pantoja D, de Lorenzo V. The Entner-Doudoroff pathway empowers
349 *Pseudomonas putida* KT2440 with a high tolerance to oxidative stress. Environ Microbiol. 2013
350 Jun;15(6):1772-85. doi: 10.1111/1462-2920.12069.

- 351 Chen MJ, Tang HY, Chiang ML. Effects of heat, cold, acid and bile salt adaptations on the stress
352 tolerance and protein expression of kefir-isolated probiotic *Lactobacillus kefiranofaciens* M1. Food
353 Microbiol. 2017 Sep;66:20-27. doi: 10.1016/j.fm.2017.03.020.
- 354 Cuzzi B, Herasimenka Y, Silipo A, Lanzetta R, Liut G, Rizzo R, Cescutti P. Versatility of the *Burkholderia*
355 *cepacia* complex for the biosynthesis of exopolysaccharides: a comparative structural investigation.
356 PLoS One. 2014 Apr 10;9(4):e94372. doi: 10.1371/journal.pone.0094372.
- 357 Ge X, Wang W, Han Y, Wang J, Xiong X, Zhang W. *Methylovorus* sp. MP688 exopolysaccharides
358 contribute to oxidative defense and bacterial survival under adverse condition. World J Microbiol
359 Biotechnol. 2013 Dec;29(12):2249-58. doi: 10.1007/s11274-013-1391-4.
- 360 Hector RE, Mertens JA, Bowman MJ, Nichols NN, Cotta MA, Hughes SR. *Saccharomyces cerevisiae*
361 engineered for xylose metabolism requires gluconeogenesis and the oxidative branch of the pentose
362 phosphate pathway for aerobic xylose assimilation. Yeast. 2011 Sep;28(9):645-60. doi:
363 10.1002/yea.1893.
- 364 Imada A, Kitano K, Kintaka K, Muroi M, Asai M. Sulfazecin and isosulfazecin, novel β -lactam
365 antibiotics of bacterial origin. 1981. Nature 289:590–591. <https://doi.org/10.1038/289590a0>.
- 366 Jitprasutwit S, Ong C, Juntawieng N, Ooi WF, Hemsley CM, Vattanaviboon P, Titball RW, Tan P,
367 Korbsrisate S. Transcriptional profiles of *Burkholderia pseudomallei* reveal the direct and indirect
368 roles of Sigma E under oxidative stress conditions. BMC Genomics. 2014 Sep 12;15:787. doi:
369 10.1186/1471-2164-15-787.
- 370 Kallifidas D, Thomas D, Doughty P, Paget MS. The sigmaR regulon of *Streptomyces coelicolor* A32
371 reveals a key role in protein quality control during disulphide stress. Microbiology. 2010 Jun;156(Pt
372 6):1661-72. doi: 10.1099/mic.0.037804-0.

- 373 Kintaka K, Haibara K, Asai M, Imada A. Isosulfazecin, a new beta-lactam antibiotic, produced by an
374 acidophilic pseudomonad. Fermentation, isolation and characterization. *J Antibiot (Tokyo)*. 1981
375 Sep;34(9):1081-9.
- 376 Lardi M, Aguilar C, Pedrioli A, Omasits U, Suppiger A, Cárcamo-Oyarce G, Schmid N, Ahrens CH, Eberl
377 L, Pessi G. σ 54-Dependent Response to Nitrogen Limitation and Virulence in *Burkholderia*
378 *cenocypacia* Strain H111. *Appl Environ Microbiol*. 2015 Jun 15;81(12):4077-89. doi:
379 10.1128/AEM.00694-15.
- 380 Li X, Wang J, Li S, Ji J, Wang W, Yang K. ScbR- and ScbR2-mediated signal transduction networks
381 coordinate complex physiological responses in *Streptomyces coelicolor*. *Sci Rep*. 2015 Oct 7;5:14831.
382 doi: 10.1038/srep14831.
- 383 Liu Y, Orsi RH, Boor KJ, Wiedmann M, Guariglia-Oropeza V. Home Alone: Elimination of All but One
384 Alternative Sigma Factor in *Listeria monocytogenes* Allows Prediction of New Roles for σ B. *Front*
385 *Microbiol*. 2017 Oct 11;8:1910. doi: 10.3389/fmicb.2017.01910.
- 386 Loveridge EJ, Jones C, Bull MJ, Moody SC, Kahl MW, Khan Z, Neilson L, Tomeva M, Adams SE, Wood
387 AC, Rodriguez-Martin D, Pinel I, Parkhill J, Mahenthiralingam E, Crosby J. Reclassification of the
388 Specialized Metabolite Producer *Pseudomonas mesoacidophila* ATCC 31433 as a Member of the
389 *Burkholderia cepacia* Complex. *J Bacteriol*. 2017 Jun 13;199(13). pii: e00125-17. doi:
390 10.1128/JB.00125-17.
- 391 Mangalea MR, Plumley BA, Borlee BR. Nitrate Sensing and Metabolism Inhibit Biofilm Formation in
392 the Opportunistic Pathogen *Burkholderia pseudomallei* by Reducing the Intracellular Concentration
393 of c-di-GMP. *Front Microbiol*. 2017 Jul 25;8:1353. doi: 10.3389/fmicb.2017.01353.
- 394 Paksanont S, Sintiprungrat K, Yimthin T, Pumirat P, Peacock SJ, Chantratita N. Effect of temperature
395 on *Burkholderia pseudomallei* growth, proteomic changes, motility and resistance to stress
396 environments. *Sci Rep*. 2018 Jun 15;8(1):9167. doi: 10.1038/s41598-018-27356-7.

- 397 Pumirat P, Saetun P, Sinchaikul S, Chen ST, Korbsrisate S, Thongboonkerd V. Altered secretome of
398 *Burkholderia pseudomallei* induced by salt stress. *Biochim Biophys Acta*. 2009 Jun;1794(6):898-904.
399 doi: 10.1016/j.bbapap.2009.01.011.
- 400 Pumirat P, Vanaporn M, Boonyuen U, Indrawattana N, Rungruengkitkun A, Chantratita N. Effects of
401 sodium chloride on heat resistance, oxidative susceptibility, motility, biofilm and plaque formation of
402 *Burkholderia pseudomallei*. *Microbiologyopen*. 2017 Aug;6(4). doi: 10.1002/mbo3.493.
- 403 Reott MA, Parker AC, Rocha ER, Smith CJ. Thioredoxins in redox maintenance and survival during
404 oxidative stress of *Bacteroides fragilis*. *J Bacteriol*. 2009 May;191(10):3384-91. doi:
405 10.1128/JB.01665-08.
- 406 Sévin DC, Stählin JN, Pollak GR, Kuehne A, Sauer U. Global Metabolic Responses to Salt Stress in
407 Fifteen Species. *PLoS One*. 2016 Feb 5;11(2):e0148888. doi: 10.1371/journal.pone.0148888.
- 408 Si M, Zhao C, Burkinshaw B, Zhang B, Wei D, Wang Y, Dong TG, Shen X. Manganese scavenging and
409 oxidative stress response mediated by type VI secretion system in *Burkholderia thailandensis*. *Proc*
410 *Natl Acad Sci U S A*. 2017 Mar 14;114(11):E2233-E2242. doi: 10.1073/pnas.1614902114.
- 411 Smith LT, Smith GM, Madkour MA. Osmoregulation in *Agrobacterium tumefaciens*: accumulation of
412 a novel disaccharide is controlled by osmotic strength and glycine betaine. *J Bacteriol*. 1990
413 Dec;172(12):6849-55.
- 414 Somprasong N, Jittawuttipoka T, Duang-Nkern J, Romsang A, Chaiyen P, Schweizer HP,
415 Vattanaviboon P, Mongkolsuk S. *Pseudomonas aeruginosa* thiol peroxidase protects against
416 hydrogen peroxide toxicity and displays atypical patterns of gene regulation. *J Bacteriol*. 2012
417 Aug;194(15):3904-12. doi: 10.1128/JB.00347-12.

418 Srivastava S, Yadav A, Seem K, Mishra S, Chaudhary V, Nautiyal CS. Effect of high temperature on
419 *Pseudomonas putida* NBRI0987 biofilm formation and expression of stress sigma factor RpoS. *Curr*
420 *Microbiol.* 2008 May;56(5):453-7. doi: 10.1007/s00284-008-9105-0.

421 **Supplementary Information Legends**

422 Table1 S1. Total Ion Chromatogram data lists. All compounds with a NIST score of 60 or more have
423 been reported with a putative identification. Where apparent multiple peaks for the same
424 compound are identified, this is due to the presence of multiple derivatives.

425 Table S2. Compounds in each sample putatively identified with a NIST score of 80 or more.

426 **Figure legends**

427 Figure 1. *B. mesoacidophila* growth changes over time under a range of conditions in nutritionally
428 replete media (LB). The charts to the left show optical density over time, with concentration of the
429 particular stressor as the third axis. The charts on the right show optical density over time, with
430 temperature as the third axis. The top panels show the growth in the presence of KCl, the middle
431 panels in the presence of diamide, and the bottom panels in the presence of H₂O₂.

432 Figure 2. *B. mesoacidophila* growth changes over time under a range of conditions in nutritionally
433 stringent media (CD85). The charts to the left show optical density over time, with concentration of
434 the particular stressor as the third axis. The charts on the right show optical density over time, with
435 temperature as the third axis. The top panels show the growth response in the presence of KCl
436 concentration, the middle panels in the presence of diamide, and the bottom panels in the presence
437 of H₂O₂.

438 Figure 3. *B. mesoacidophila* growth curves in CD85 at 30 °C with an increasing concentration of H₂O₂.
439 All conditions were performed in triplicate.

440 Figure 4. Chromatogram of one of the replicates in CD85 (without additional stress) produced in
441 OpenChrom using the Savitzky-Golay smoother and Amdis peak deconvoluter. The collection of
442 peaks at A are dominated by mannose, the peaks at B by α -D-glucoopyranoside.

443 Figure 5. Compounds putatively identified with a NIST score of 80 or higher, across all replicates in
444 each condition (CD85 in black, CD85 with 1 mmol l⁻¹ diamide in light grey, CD85 with 220 μ mol l⁻¹
445 H₂O₂ in dark grey). All sugars were identified as their derivatized forms.

446 Figure 6. Chromatogram of intracellular metabolome of *B. mesoacidophila* cells grown in CD85
447 treated with diamide showing peaks at 7.142 minutes and ~53 minutes, both of which were unique
448 to diamide treated cells. Images were generated and analysed in OpenChrom.

449

450